Colloid Polym Sci (1995) 273:2–15


LEADING CONTRIBUTION

M. Almgren
W. Brown
S. Hvidt

# Self-aggregation and phase behavior of poly(ethylene oxide)-poly(propylene oxide)-poly(ethylene oxide) block copolymers in aqueous solution

Received: 17 May 1994
Accepted: 1 July 1994

M. Almgren (✉) · W. Brown
Department of Physical Chemistry
Uppsala University
P.O. Box 532
751 21 Uppsala, Sweden

S. Hvidt
Chemistry Department
Roskilde University
4000 Roskilde, Denmark

**Abstract** The phase behavior and aggregation properties of block copolymers of poly(ethylene oxide)-poly(propylene oxide)-poly(ethylene oxide) (Pluronics, poloxamers) in aqueous solution have recently attracted much attention. Both experimental and theoretical studies are reviewed, not comprehensively, but with the focus on studies, partly cooperative, partly independent, performed by groups in Uppsala (light scattering and fluorescence), Roskilde (rheology and calorimetry), Risø (SANS), Graz (x-ray and speed of sound), and Lund (theoretical model calculations).

The phase behavior of these copolymers is similar in many respects to that of conventional non-ionic surfactants, with the appearance of hexagonal, cubic, and lamellar liquid crystalline phases at high concentrations. In the isotropic solution phase the critical concentration for micelle formation is strongly temperature dependent, and at a given concentration the monomer to micelle transition occurs gradually over a broad temperature range, partly due to the broad size polydispersity of both the PO- and EO-blocks. For some Pluronic copolymers a transition from globular to long rod-like micelles occurs above a transition temperature, resulting in a strong and sudden increase of viscosity and viscoelasticity of the solution.

Size and aggregation numbers have been determined for the globular micelles in some cases, and also the rod-like micelles have been characterized. NMR and fluorescence measurements have provided further information on the properties of the micellar core and mantle. In combination, results from different measurements on the same Pluronics material indicate that the aggregation number of the micelles increases with the temperature, whereas the hydrodynmic radius varies much less. The PEO-mantle of the micelles seems to contract with increasing temperature. The core appears to contain appreciable amounts of PEO in addition to PPO (and also some water). The segregation between core and mantle is not as distinct as in normal micelles, a conclusion which is in line with the predictions from the model calculations.

**Key words** Blockcopolymer – poly(ethylene oxide) poly(propylene oxide) – light scattering – fluorescence – aggregation – micelle – phase behavior

## Introduction

The physical chemistry of self-aggregation has developed into a central area of research with timely problems of both theoretical and experimental character, and with both practical and fundamental consequences in physics, chemistry, biology, and medicine. Already the simplest surfactants display a complex and intriguing aggregation behavior which now is quite well understood, and even more complex systems are being studied intensively, e.g. those involving interactions between polymers and surfactants [1, 2], or block copolymers which form micelle-like aggregate in selective solvents [3].

Poly(ethylene oxide)-poly(propylene oxide)-poly(ethylene oxide) block copolymers, called Pluronic or Synperonic commercially, are in many respects similar to nonionic surfactants in aqueous solution, displaying clouding at high temperatures and aggregation into micelles and liquid crystalline phases at lower temperatures and at higher concentrations. The phase and aggregation behavior is strikingly dependent on temperature, concentration, and composition of the copolymers. The aggregation leads to unusual and potentially useful rheological properties, for instance the formation of a rigid gel for some Pluronic polymers, at concentrations above 20–30% by weight depending on copolymer composition, which passes into a fluid solution at both high and low (inverse melting) temperatures. Some Pluronic copolymers also attain gel-like properties at high temperatures in dilute solution.

Regarded as polymers, the Pluronic copolymers are of small size. The central PO-block gives the hydrophobic driving force for aggregation, just as the alkyl chains of usual surfactants, but to give a comparable free-energy gain on aggregation, the PO-block must be much longer than the alkyl tail of a normal surfactant. The unimers and the micelles of the block copolymers are therefore much larger than surfactant monomers and micelles with a typical micelle radius of the order of 60–120 Å compared to 20–30 Å for globular surfactant micelles. Normal nonionic surfactants of the $C_xE_y$-type ($C_xH_{2x+1}(OCH_3CH_2)_yOH$) form micelles in which the segregation in the core is almost complete so that it consists almost exclusively of the alkyl chains, with very little water or head groups present inside the interface. It is considered that the PPO chains are less exclusive, and an important question is to what extent water and EO-groups are present in the core.

Another difference between the Pluronic copolymers and normal surfactants is the triblock structure. This feature seems to be less important for the general properties, presumably because the long PO block effectively decouples the two hydrophilic portions of the polymer: it does not behave as a boloform surfactant, i.e., one with hydrophilic heads at both ends. More important is the fact that the Pluronics are only available as polydisperse preparations which contain appreciable amounts of both diblock material and free PO chains in addition to the main component. These impurities are difficult to remove and, as will be discussed below, a number of peculiarities and conflicting observations in early studies can be attributed to the use of impure samples.

This overview will be mainly concerned with the results from studies from our groups, using fluorescence methods (Almgren), scattering methods (Brown), and rheological and calorimetric methods (Hvidt). Our studies on Pluronic copolymers started in 1987 when P. Bahadur was visiting Uppsala. Later on, other laboratories became involved, and an interest in these systems developed simultaneously in many other places. In Lund, the model calculations by Linse have been particularly enlightening, and will be discussed below. Similar models have been developed independently by Hurter et al. [4].

This review will start with a brief presentation of the solution properties and the phase behavior. After a discussion of the theoretical models, the properties of the micelles, and the dependence of aggregation on temperature, composition, and solvent will be considered in some detail.

## Solution properties and phase diagram

Figure 1 displays the water-rich part of a tentative and schematic phase diagram for P85 (average composition $E_{27}P_{39}E_{27}$), based on results from several different investigations. Very similar diagrams have been presented for P85 [5] and for P-94 ($E_{21}P_{47}E_{21}$) [6]. Outside a large $L_1$-area containing monomers at low temperature and micelles at higher temperatures, liquid crystalline phases form at concentrations above 25% by weight.

An $I_1$ cubic phase, comprising closed, globular aggregates, and an hexagonal phase have been identified [7]; other phases (lamellar, cubic $V_1$) are probably also present [8]. In dilute solution, clouding (here separation into two $L_1$-phases) occurs at a temperature of about 83 °C; the cloud point increases with concentration for P85, but is almost independent of concentration for P94. A maximum occurs on the cloud point curve above the hexagonal phase. This is an artefact, probably due to that a lamellar phase is also present in this region.

Structural transitions occur within the $L_1$-area, as evidenced by large changes in rheological and other properties. On heating a stirred solution, a dramatic increase in viscosity occurs, and viscoelasticity and gel-like solution properties emerge suddenly at a temperature below the

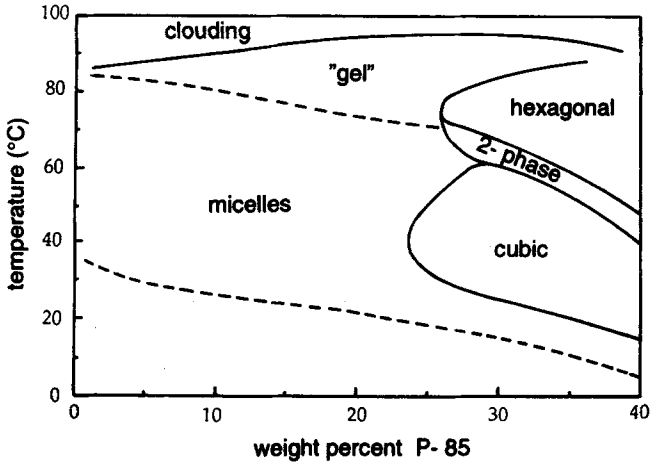


**Fig. 1** Schematic phase diagram for P85-water, at water rich compositions. The borders to the cubic, and in particular the hexagonal liquid crystalline phases are tentative. The broken lines within the isotropic solution phase indicate transition temperatures from monomers to micelles (lower line; this is the temperature for the maximum rate of micelle formation) and the transition to rod-like micelles, which turns the solution into a gel (upper line).

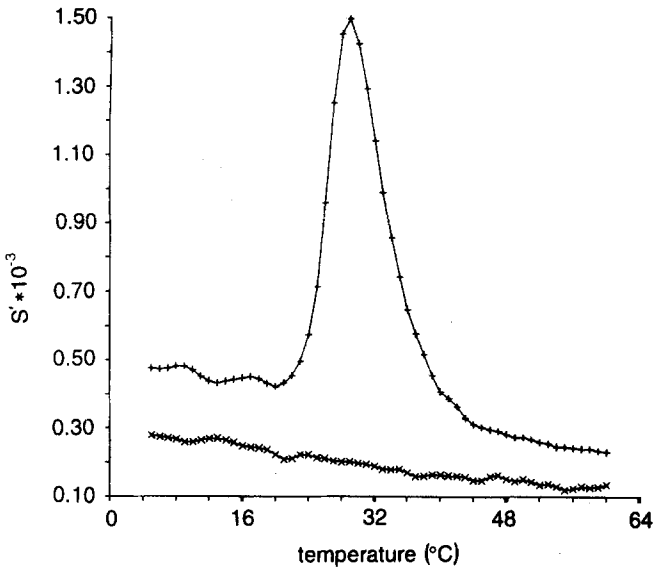


**Fig. 2** The negative first derivative of the specific speed of sound, $S' = -dS_s/dT$, as a function of temperature for 5 wt% P85 solution ( + + + ) and a 10 wt% sucrose solution ( × × × ). The specific speed of sound is defined as $S_s = (S_{solution} - S_{aq})/S_{aq}$, and increases with the number of particles in the solution. (Reproduced with permission from ref. [11]).

cloud-point. This concentration-dependent transition temperature is shown in Fig. 1 as the upper broken line. It was determined from rheological measurements as the gelation point where $G'$ and $G''$ become equal. $G'$ the elastic storage modulus, and $G''$, the loss modulus, are measures of the energy stored as elastic energy and the energy lost as heat, respectively, during an oscillatory deformation. Very similar results for the transition temperature have been obtained by visual observation of the onset of "high" viscosity [9]. The fact that these properties are observed at very low concentrations indicates that long rods, or thread-like aggregates must be present, a finding which is also corroborated by the emergence of an hexagonal phase at high concentrations and temperatures. Furthermore, fluorescence quenching results from a 5% solution show that growth occurs, from aggregation numbers of 60 at 40 °C to large aggregates with a quenching behavior typical for long cylinders at 70 °C and above [10].

The broken line at lower temperature indicates the midpoint of a broad temperature range over which the transition from unimers to micelles occurs. The transition is monitored very precisely by an interesting technique based on the determination of the speed of sound in the system [11]. At constant solute concentration, the speed of sound decreases when the number of particles decreases, as occurs on micellization, and Glatter showed that the rate of change of the speed of sound with temperature can be measured to provide a distinct and well-defined peak (Fig. 2). The temperature at which the maximum rate of micelle formation occurs according to this method [5] is shown as the broken line in the phase diagram. Micelle formation starts already at a temperature about 10 degrees lower and the change continues to temperatures well above the maximum rate point. Results in very good agreement were obtained also by DSC (differential scanning calorimetry) and other methods [5].

Micelle formation is thus a much more gradual transition for the Pluronics than for usual nonionic surfactants. This may in part be due to the fact that the polymers are polydisperse in composition, but probably more important is the fact that the change with temperature from hydrophilic to hydrophobic occurs much more gradually for the short PO-blocks than for typical high polymers. Hvidt et al. [6] compared DSC data for P94 with those for a PPO fraction of about similar size as the PO block in P94. The onset and the peak of the transition occurred in both cases at close to the same temperature. The temperature dependence of micellization for these substances is thus determined primarily by the PPO-block length, whereas the decrease of the hydrophilicity of the PEO blocks is less important. For nonionic surfactants, only the latter effect is observed; the solubility in water of alkylchains such as those found in normal surfactants depends little on temperature, and often shows a minimum close to room temperature [12].

Scattered data are available from many other systems with regard to different features of the phase diagrams. Copolymers with the same PO-block size as P85 but with longer EO-blocks ($E_xP_yE_x$: F87; $x = 67$, F88; $x = 96$ with $y = 39$) have been studied, as well as one, L81, having very short EO-blocks ($x = 6$). In this series, it was found that

the cubic phase starts to form at a lower concentration and has a wider stability range the longer the PEO-blocks [13, 14]. In the case of L64, ($E_{13}P_{30}E_{13}$). there is no indication of gel-formation (at least not below 30%) and no abrupt viscosity increase at high temperature below the cloudpoint at low concentrations. Micelle formation in L64 requires higher temperature and occurs less readily than in P85, showing that the size of the hydrophobic PO-block is more important for the aggregation than the relative sizes of the blocks [15].

The boundaries and assignments of the lyotropic liquid crystalline phases are still tentative or incomplete. The boundary between the solution and the cubic phase, which Mortensen describes as BCC-packing of globular micelles [7], may be determined accurately by several techniques [5]. The rheological results for P94 of Hvidt et al. [6] are particularly striking. Figure 3 shows the temperature variation of $G'$ and $G''$ for 25.5 wt% P94 as compared to 29.7 wt% PEO-6000. The PEO solution is Newtonian, with a $G''$ which far exceeds $G'$ at all temperatures. At low temperatures the P94 solution behaves similarily, but at 26 °C $G'$ increases abruptly and reaches much larger values than $G''$. The solution undergoes a transition to a hard gel, which can be identified with the cubic phase. At 40 °C both $G'$ and $G''$ decrease rapidly, and between 48° and 58 °C a viscoelastic solution is again formed since $G'' > G'$. A second gel structure is again formed at temperatures above 58 °C, referred to as a "soft" gel, since its elastic modulus is more than two orders of magnitude smaller than that of the "hard" gel at lower temperature. At high concentrations the soft gel is at conditions where a hexagonal phase is expected.

Figure 4 show the temperature variation of $G'$ at different concentrations. It is obvious that the formation and melting of the gels may be determined very precisely. At 27% a new maximum in $G'$ appears at 55 °C, between the hard and the soft gel, which may be taken as evidence for the formation of a new intermediate phase. At concentrations below 24.5% the hard gel does not form, but the "soft gel" persists down to very low concentrations, where it should be taken as an indication for the formation of long rod-like micelles, as discussed above, and not a hexagonal phase.

One of the characteristics of an hexagonal phase is optical birefringence. At 75 °C, flow birefringence (under shear stress) was observed at concentrations of 15, 20, and 25% P85, whereas at 27.5% the sample is birefringent without a shearing stress [16]. These results show that the boundary to the hexagonal phase is close to 27.5% at 75 °C, and that the rodlike micelles at lower concentrations orient due to the shear stress.

It is interesting to observe that an increase of pressure causes decomposition of the micelles into monomer and thus (inverse) melting of the cubic phase (in analogy with decreasing the temperature) [17]. This situation is summarized in Fig. 5 showing how the micellar volume fraction decreases with increasing pressure due to dissociation of micelles, whereas the opposite trend is seen on increasing temperature.

Before discussing in detail the properties of the micelles in these systems, we shall devote a section to the advances in the theoretical modeling of the systems, from which a deeper understanding may be gained.

**Fig. 3** Viscoelastic properties of 25.5 wt% P94 and 29.7 wt% PEO-6000 solutions as a function of temperature at 0.05 Hz. For PEO $G''$ is shown (filled squares) and for P94 $G''$ (open circles) and $G'$ (filled circles). H and S mark "hard" and "soft" gels, respectively. (Reproduced with permission from ref. [6])

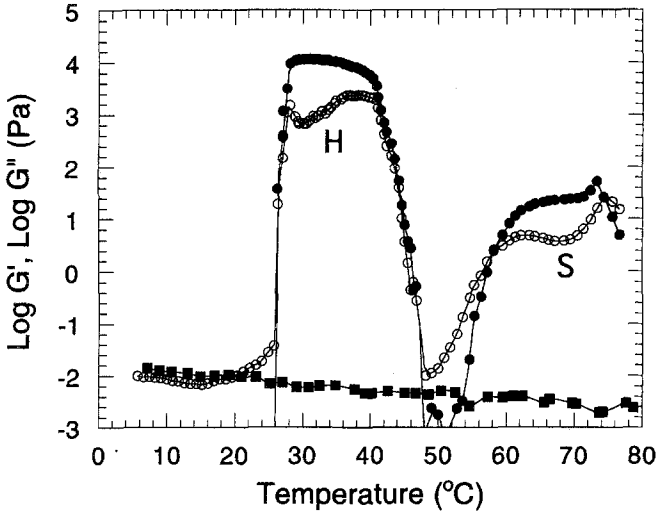


**Fig. 4** $G'$ at 0.05 Hz for P94 at concentrations (wt%): 6.3 (filled triangles); 24.7 (filled squares); 25.0 (open squares); 27.0 (filled circles); 32.0 (open circles). H and S mark "hard" and "soft" gels, respectively. data replotted from ref. [6]

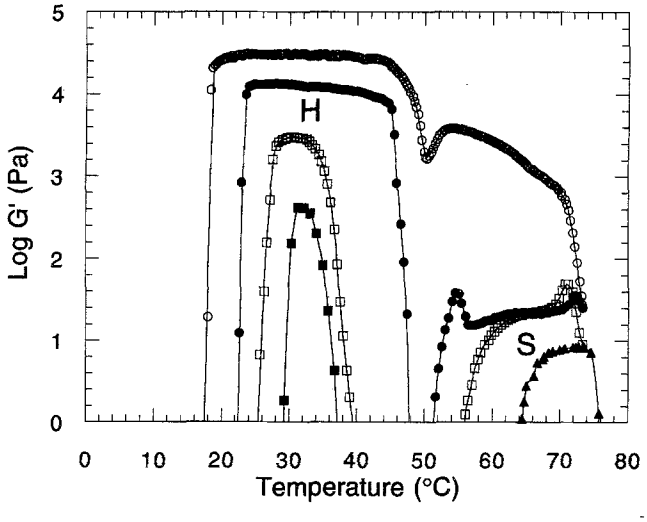

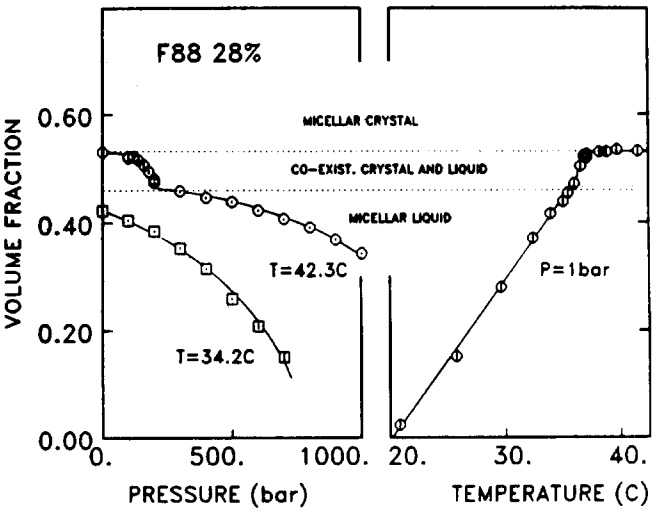


**Fig. 5** Pressure and temperature dependence of the volume fraction of micelles, as determined from SANS studies, for F88 at 28 wt%. (Reproduced with permission from ref. [17]).

## Theory and models

Major questions to consider are why self-aggregation occurs at all in the systems, and why clouding occurs with increasing temperature. The behavior of PEO and PPO polymers in aqueous solution will first be considered.

PEO is probably the best studied of all water-soluble synthetic polymers. Most striking among its solution properties is the clouding behaviour, i.e., that the solubility of the polymer is drastically reduced above a certain temperature so that two phases coexist, one dilute and one concentrated.

Several explanations have been suggested for the occurrence of a lower consolute temperature (LCT) for PEO. Obviously, the polymer-polymer interactions become relatively more favorable, and the polymer-water interactions less favorable with increasing temperature. Kjellander et al. [18] suggested an explanation based on the properties of water: the polyethylene oxide chain was proposed to fit well into the structure of fluid water at ambient temperature. With increasing temperature the water structure diminishes and the compatibility of the polymer with water disappears. This suggestion would explain why neither poly(methylene oxide) nor poly(propylene oxide) are water-soluble to any appreciable extent (although moderately long PPO oxide polymers are water-soluble at low temperature). Attractive as it may seem, this theory is not tenable. For one thing, the clouding behavior of PEO is not only seen in water, but in several other polar solvents as well [19].

A second explanation utilizes hydrogen-bonding between the ether oxygens and water: the hydrogen bonded state is stabilized in water, but as the temperature is raised the hydrogen-bonds are broken, resulting in more favorable polymer-polymer interactions. There is at least one report on clouding of PEO in a very weakly hydrogen-bonding solvent, *tert*-butyl-acetate [20] which does not fit this hypothesis. Furthermore, if this explanation is correct, poly(methylene oxide) should be water-soluble and display clouding.

A third model considers the conformational properties of the polymer chain. Karlström [21] suggested, based on a quantum chemical analysis of the conformational equilibrium of a molecule containing an –OCCO– sequence [22], that, of the possible conformations from rotation around the C–C bond, the majority are relatively non-polar trans conformers, with no or only a small residual dipole moment, whereas essentially only two gauche conformers are strongly polar. These conformers have the lowest energies and interact most favorably with water. With increasing temperature the non-polar conformers are favored, and since they are much more numerous they will start to dominate the properties of the chain, making interactions with water less favorable. $^{13}C$ NMR chemical shift studies of PEO in water [23] have shown the non-polar trans conformers to be favored at high temperatures, as predicted.

Karlström [21] also incorporated this two-state polymer model into a Flory–Huggins type of theory and was able to reproduce the phase diagram of PEO-water in a qualitative way with energy and statistical parameters as given in Table 1. More importantly, the theory also gives a good qualitative explanation for other effects, e.g., the

**Table 1** Internal state parameters (energy $U_{AB}$ and statistical weight $g_{AB}$) and Flory–Huggins interaction parameters ($\chi_{BB'}$) used in Linse's theoretical model. Energy in kJ mole$^{-1}$.

| Species | State | State no. | $U_{AB}$ | $\chi_{BB'}$ |
|---|---|---|---|---|
| water | | 1 | 0 | 1 |
| EO | polar | 2 | 0[a] | 1[a] |
| | nonpolar | 3 | 5.086[a] | 8[a] |
| PO | polar | 4 | 0[b] | 1[b] |
| | nonpolar | 5 | 11.5[b] | 60[b] |

| | $kT\chi_{BB'}$ | | | |
|---|---|---|---|---|
| State no. | 2 | 3 | 4 | 5 |
| 1 | 0.6508[a] | 5.568[a] | 1.7[b] | 8.5[b] |
| 2 | | 1.266[a] | 1.8[c] | 3.0[c] |
| 3 | | | 0.5[c] | −2.0[c] |
| 4 | | | | 0.4[b] |

[a] From a fit to data for the PEO-water system, ref. [21]
[b] From a fit to data for the PPO-water system, ref. [26]
[c] From a fit to data for the ternary PPO-PEO-water system, ref. [24, 25]

interactions of the polymer with other substances, and it also works for a number of other non-ionic polymers which contain the –OCCO– sequence, notably PPO and water-soluble cellulose derivatives.

The low solubility of PPO in water is explained by the fact that the lower consolute temperature (LCT) is below the freezing-point for large polymers; only short oligomers have appreciable water-solubility with an LCT above room temperature. With the Flory–Huggins parameters chosen as in Table 1, the phase diagram is qualitatively well modeled [22].

The three-component phase diagram of PPO-PEO-water could be modeled in a similar way [24], with the interaction parameters between PPO and PEO given in Table 1 [25]. Using the Flory–Huggins descriptions of PPO and PEO, Linse and Björling [26] developed a lattice theory for adsorption and micelle formation in PEO-PPO-PEO block-copolymers, built on the frame-work set by Scheutens and Fleer [27]. Of special interest in the present connection is the modeling of micelles and micelle formation by Linse and Malmsten [28] and Linse [25, 29]. They calculated the temperature dependence of the CMC, the hydrodynamic radius, and aggregation numbers as a function of temperature and concentrations, and also the distribution of PO and EO segments as a function of the distance from the center of the micelle. As far as comparisons with experiment are possible, qualitative agreement is found; some features, however, are expected to be less well accounted for in this model. In particular, the authors point out that models of this type seem to predict more water in the core of the structure than is experimentally found.

In the first calculations [25, 28] globular micelles were the only aggregates considered; allowance for cylindrical structures was made in a later paper [29]. For Pluronics with short EO-blocks, like $E_6P_{37}E_6$ (data from [30]), the clouding behavior was quite well described already in the first calculations, but not for P85 and several other copolymers with larger EO blocks. For these, the coexistence curves occur at lower temperature in the model than in reality. Furthermore, experiments on P85 (but not P94) show an increase in the cloud point with increasing concentration, which is opposite to the predicted behavior. The later calculations show that rodlike micelles are stable at higher temperatures in a region which was assigned to the two-phase area in the first calculations and with a concentration independent transition temperature in the two-phase region. An example of a calculated phase diagram, for P104 ($E_xP_yE_x$; $x = 25$, $y = 56$), is reproduced in Fig. 6. The correct ordering of the structures is obtained, and from a comparison of models for P105 ($x = 37$, $y = 25$), P95 ($x = 31$, $y = 47$), and P104 there is also an indication that with shorter EO-blocks higher concentrations are

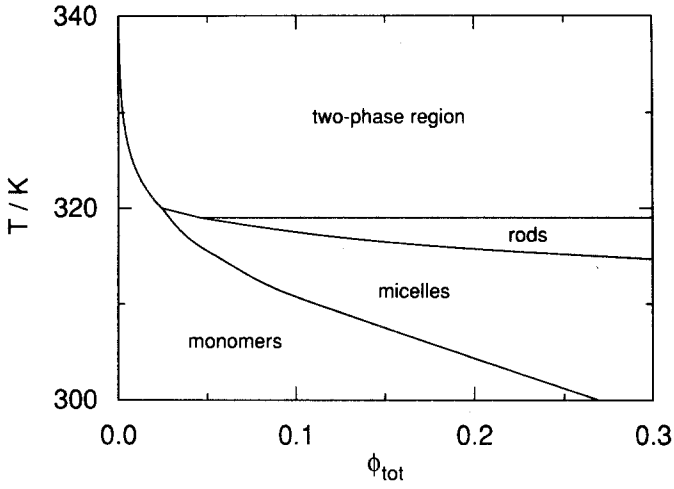


**Fig. 6** Calculated phase diagram for a copolymer corresponding to P104 ($E_{25}P_{56}E_{25}$). The model is described in the text. (Reproduced with permission from ref. [29]. Copyright [1993] American Chemical Society)

required for the rods to become stable with respect to globular micelles [29].

The temperature at which micelle formation occurs, the CMT, decreases with concentration in a way that is well described by the model calculations, but in real systems the aggregation starts at much lower temperature than predicted. It is possible that the PO-rich impurities in the samples are of importance for this effect, as for the creation of the very broad monomer-to-micelle transition region. Also, the influence of impurities and polydispersity was recently treated by Linse [31, 32]. It was found that the copolymer polydispersity could explain the early onset of micelle formation.

The phase separation (clouding) is predicted to occur at too low temperatures [25]. It should be noted that no interactions were assumed between the structures in the calculations, and that phase separation was assumed to result in a dilute unimer solution and a non-structured concentrated phase, not in two micellar solutions as is usually found in Pluronic solutions, as well as in normal nonionic surfactant solutions. If interactions between the aggregates were taken into account, it could be expected, perhaps naively, that the aggregates with their exposed PEO groups should interact in a manner similar to PEO itself and display a higher cloudpoint than that predicted in the present calculations, where the PPO blocks also play a significant role. To account for the cubic phase at high concentrations it is, of course, also necessary to introduce repulsive micelle-micelle interactions.

Linse et al. have also calculated the segment distribution in the micelles, which is particularly interesting since this information is very difficult to obtain experimentally;

only the consistency of experimental results with the calculated distributions can be indirectly assessed. An example is presented in Fig. 7. The total volume fraction of polymer is almost constant in the innermost layers, leaving a volume fraction of about 15% for water, and although this fraction probably is overestimated in this type of model [25], there is reason to assume that appreciable amounts of water are present in the core. The total polymer volume fraction starts to decrease above a layer number (the layer number is proportional to the radius) which increases with temperature, and then falls gradually and slowly. The transition to rod-like micelles results in the distinct decrease in the core radius. The PO and EO segment distributions show that there are appreciable amounts of EO groups in the core, and that the interpenetration increases with temperature, and is only slightly reduced on the transition to rods. The usual picture of a micelle as consisting of a core composed almost exclusively of the hydrophobic groups and outside that a mantle with the hydrophilic groups and water is apparently not valid. This is a very interesting prediction which will be discussed in the light of experimental results below. In hindsight, it should not be a surprise. The separation of PPO from water above the cloudpoint in the PPO-water system is certainly not complete; a fraction of water should then be also present in the core of PPO. From the three-component phase diagram of PPO-PEO-water [25] it is obvious that the PPO-PEO interactions are much less segregative than alkyl-PEO, allowing an appreciable intermixing.

**Fig. 7** Calculated segment volume fraction ($\phi_{EO,i}$, $\phi_{PO,i}$, and the sum) versus layer number (i) for a total volume fraction $\phi_{tot} = 0.0528$ at $T = 320$ K (at the CMC, solid curves) and at T = 335 K (above the CMC, dashed curves) for a model corresponding to F127 ($E_{99}P_{65}E_{99}$). The calculated aggregation numbers are 6.6 and 36.2, and the hydrodynamic radii 12.2 and 19.8 (layers), respectively. (Adapted with permission from ref. [25]. Copyright [1993] American Chemical Society.)

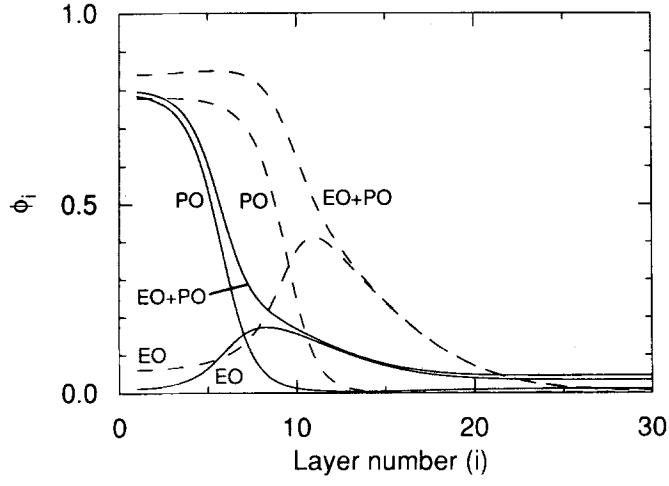


## Micelle formation

Determination of the concentration and temperature at which micelle formation starts often gives conflicting results. Some reasons for this are the strong temperature dependence of micellization, which is most marked at low concentrations, the broad temperature range for the monomer-micelle transition, and the polydispersity of the samples, in particular, the presence of both diblock material and free PPO chains.

The CMT is represented as the broader line between monomers and micelles in the calculated diagram of Fig. 6. The broken line in Fig. 1 represents the maximum rate of micelle formation. Calculations show that the CMT increases rapidly on dilution at low concentration. Although not shown in Fig. 1, measurements on P94 [6] show that the CMT increases strongly at low concentration.

The fact that micelle formation occurs gradually over a broad range of temperature means that different results are obtained depending on the sensitivity of the particular method to the onset of micelle formation. Further uncertainty is produced when diblock copolymers and free PPO chains are present, which seem to be the rule in commercial preparations [6]. These more hydrophobic molecules start to aggregate or precipitate at concentrations and temperatures below the onset of proper micellization. In experiments where the micellization is monitored by the use of hydrophobic probes, for example, pyrene, for which a change of fluorescence occurs between polar and nonpolar environments, the formation of even very minute amounts of hydrophobic domains may be sufficient to indicate micelle formation. Early results using pyrene were interpreted in terms of solubilization in "unimer" micelles [33], but solubilization in aggregates formed from impurities appears a better and more consistent explanation [34]. Light-scattering studies also show an anomalous increase of the scattering intensity at low concentrations and temperatures which can be ascribed to the presence of such impurities. [35, 36].

The progressive nature of micelle formation is clearly shown in Laplace-inversion relaxation time distributions from DLS measurements, as exemplified in Figs. 8 and 9 for P85 [36]; very similar results have been obtained for F87 and F88 [13]. The results on P85 pertain to a sample which was later shown to contain appreciable amounts of hydrophobic impurities. The slow peak with substantial amplitude that appears at low concentration and temperature (the lowest concentrations at 10° and 15 °C in Fig. 8) is probably related to the hydrophobic diblock and PPO impurities; the amplitude was somewhat reduced in purified samples (prepared by refluxing with hexane). Although the peak is prominent, only a small fraction of the

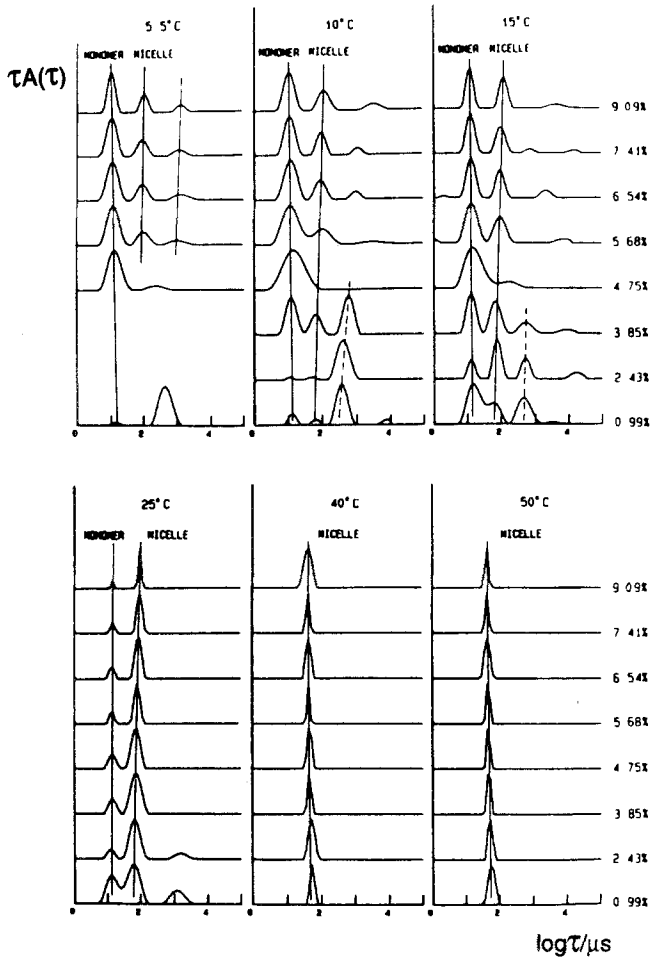


**Fig. 8** Inverse Laplace transform relaxation time distributions from DLS measurements at angle 130° for P85 at low concentrations and temperatures between 5° and 50 °C. Peaks attributed to monomers and micelles are indicated in addition to peaks at low concentrations which probably represent clusters involving PPO and diblock contaminants. (Reproduced with permission from ref. [36]. Copyright [1991] American Chemical Society.)

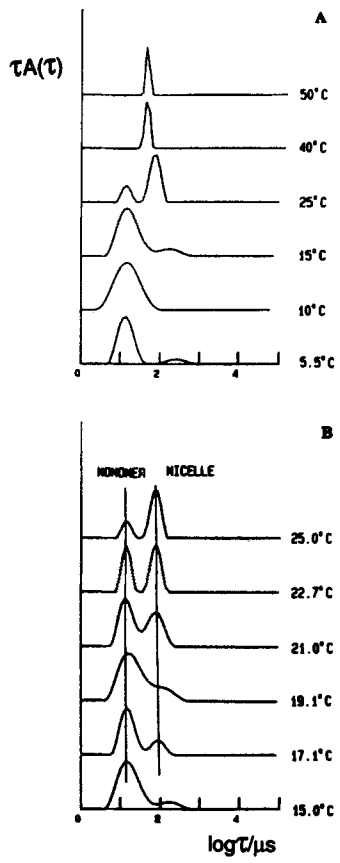


**Fig. 9** ILT relaxation time distributions in the temperature range of the monomer to micelle transition at 4.8 wt% of P85. (Reproduced with permission from ref. [36]. Copyright [1991] American Chemical Society.)

mass, united into large aggregates, is required to produce it. It is possible that these large features, with hydrodynamic radii in the range of 300–3000 Å [13], may be regarded as disperse particles of PPO, stabilized from precipitation by adsorbed diblock and triblock copolymers.

At temperatures of 25 °C and below, and concentrations below 10%, a peak representing free monomer is evident in the relaxation time distributions. Figure 9 shows how the monomer peak is successively replaced by micelles on increase of the temperature for a 4.8% sample; at 40 °C and above only micelles are seen as a clean narrow peak. The monomer-micelle transition range appears from these measurements to extend from about 15 °C to somewhere between 25 and 40 °C, which is in good agreement with the range indicated by DSC and the speed of sound measurements discussed above.

In P85, as well as in F87 and F88 [13], the relaxation time spectrum at 40° and 50 °C shows a single narrow peak over a wide range of concentration extending from dilute solution, where the relaxation rate represents the diffusion of individual micelles as discussed above, to well into the cubic phase, where a different interpretation of the dynamical behavior is clearly required.

## Micelle size and composition

From the DLS data at low concentrations the hydrodynamic radius, $R_H$, of monomers and micelles can be calculated from an extrapolation to zero concentration [13, 36]. Some results are collected in Table 2. For P85, the self-diffusion coefficient as determined by the pulsed field gradient NMR method [37] gave a somewhat lower value for the hydrodynamic radius at infinite dilution than DLS

( ≈ 80 Å from DLS at 25 °C, 71 Å from NMR at 24.5 °C). In DLS monomers and micelles are distinguished in the relaxation time distribution and a $z$-average dimension is obtained for each. With NMR measurements, on the other hand, the diffusion coefficient is close to the number average. Thus, the monomer is averaged over its motion both as a free entity and in the micelles (a single exponential decay of the echo amplitude was noted in this study, showing that on the NMR timescale the monomer exchanges rapidly between micelles and the solution). This explains the lower D-values from NMR, particularly at low temperatures where the monomer is the dominant species in the solution. Furthermore, the extrapolation to zero concentration is an ambiguous procedure under these circumstances, when a progressive change towards a larger fraction of monomers occurs on dilution.

From the results in Table 2 the hydrodynamic size of both monomers and micelles is seen to vary regularly with the size of the copolymers (or the size of the PEO blocks in this series). The hydrodynamic radius of the micelle decreases with increasing temperature, at least for F87 and F88. This does not imply that the aggregation numbers decrease; rather it is an indication that the EO-mantle contracts with increasing temperature, as has earlier been observed for another poloxamer [38].

The hydrodynamic radius from the DLS measurements cannot be readily converted to an aggregation number or molecular weight of the micelle. There have been attempts to determine the molecular weight from static light scattering, SLS. The classical procedure, involving an extrapolation to zero concentration, can be ambiguous, for example, in systems displaying a complex association behavior as shown by the relaxation time distributions in the present systems. Usually, the results from SLS give too low aggregation numbers which are incompatible with results from other types of measurement. This may be so even when, as in the study of L64 [15], it was possible to correctly estimate the concentration of micellized L64 by subtraction of the amount of free monomer in the solution.

**Table 2** Hydrodynamic radii from DLS and NMR measurements on monomers and micelles of some Pluronics in water.

| Pluronics | Hydrodynamic radius (Å) Monomer | micelle |
|---|---|---|
| L81 | 15[as] | |
| P85 | 18[b] | 93[b](15°); 80[b](25–50°); 62[c](21°); 71[c](25°); 90[c](36°) |
| F87 | 24[a] | 106[a](40°); 82[a](50°) |
| F88 | 29[a] | 131[a](40°); 105[a](50°) |
| L64 | 15–18[d] | 65[d](NMR, 40°); 60–80[d](DLS, 40°) |
| F68 | 22–25[e] | 75[e](NMR, 40°); 85[e](DLS, 41°) |

[a] ref. [13]; [b] ref. [36]; [c] ref. [36], PFG-NMR; [d] ref. [15]; [e] ref. [49]

The free and micellized fractions were estimated from NMR self-diffusion measurements, with the results shown in Fig. 10. Notable in those results is the gradual increase in the amount of free L64, from a value of 0.35% by weight at the CMC (0.4%), to a stable level of about 0.85% at high concentrations. Such an increase has also been found for nonionic surfactants with natural headgroup size distributions [39], and is easily understood from the variation of the water solubility of the homologous components. The aggregation number from the SLS was estimated as 25–30 after these corrections, at 40 °C.

In another study of L64 [40] the time-resolved fluorescence quenching method, TRFQ, was employed for determination of average aggregation numbers, but proved difficult to apply to the pure Pluronic polymers, due to slow quenching under the conditions used. An estimated aggregation number of 145 for L64 at 40 °C should be reduced by a factor of about 2 to correct for free L64 in the solution. The resulting value of about 70 is more likely correct, but still larger than the values from SLS by a factor of more than 2.

For P85 from 40° to 75 °C the DLS measurements show only a single peak due to the micelles (at higher temperature a fast peak due to the rotational motion of long rods appears as will be discussed below). Preliminary measurements of the aggregation number with both TRFQ and SLS [10, 16, 36] gave results as presented in Fig. 11, which reveal the rapid growth when the transition to rods take place. Comparison of the SLS and the TRFQ results shows again that the former gives much smaller values than the latter (at low temperatures; for rods TRFQ is expected to give too low results). The discrepancy between the results from these two methods is probably due

**Fig. 10** Concentrations of monomeric and micellized L64 as a function of the total concentration, from NMR self-diffusion measurements at 40 °C. (Reproduced with permission from ref. [15]. Copyright [1992] Academic Press.)

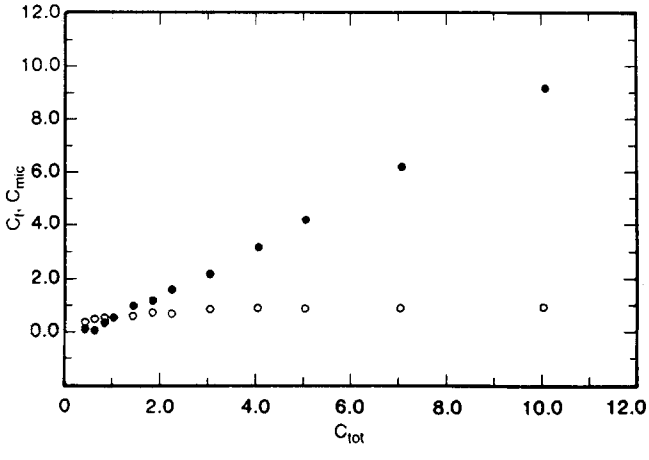

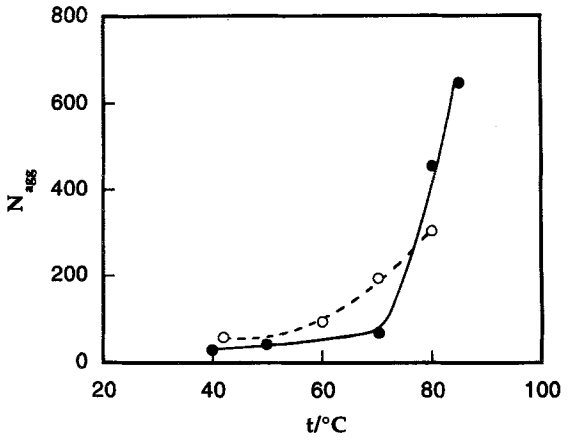


**Fig. 11** Aggregation numbers versus temperature for P85. Filled symbols: Result from static light scattering, involving extrapolation to zero concentration. Open symbols: Fluorescence quenching at 5 wt%. Data from refs. [9, 30, 35]

to the different concentration regions: the SLS results are from measurements at very low concentrations and extrapolated to zero concentration, whereas the TREQ results refers to a finite concentration of 5%. Because of the concentration dependence of the transition temperatures, the system at the higher concentration is farther from the CMT and enters the rod region earlier.

SANS measurements are another source of size information. The extensive SANS studies by Mortensen et al. [7, 14, 41, 42] on L81, P85, F87, and F88 have given consistent results over wide temperature and concentration ranges when interpreted using a model assuming a particle with dense core and an effective hard-sphere interaction between the micelles. In the Ornstein-Zernike approach, using the Percus-Yervick expression for the pair-correlation function, an analytical form is obtained for the scattering function. Fits to the experimental data results in values of the *micelle core radius*, $R_c$, the *hard-sphere interaction radius*, $R_{hs}$, and the *volume fraction of hard-spheres*, $\phi$. Some results are collected in Table 3. The hard-sphere interaction model for these micelles with their extended PEO mantles also containing water, appears somewhat oversimplified. The results, however, are consistent with the phase diagram in that the estimated hard-sphere volume fraction reaches a limiting value of about 0.53 at the temperature and concentration at which the cubic phase is formed. This volume fraction is within the coexistence range for hard-sphere fluid and solid phases, $\phi = 0.494$ to 0.545 [43, 44].

The results for the core radius from SANS, Table 3, indicate a slight increase in the radius with decreasing size of the EO-blocks, and stronger increase with increasing temperature. Both the factors result in a smaller effective size of the EO-headgroups, and from simple packing argu-

**Table 3** Core radius and hard-sphere interaction radius from SANS determinations, ref. [14].

| | Core radius (Å) | | | Hard-sphere radius (Å) | | |
|---|---|---|---|---|---|---|
| Pluronics | 20° | 40° | 50 °C | 20° | 40° | 50 °C |
| P85 | 37 | 47 | 50 | 57 | 70 | 78 |
| P87 | 30 | 45 | 49 | 50 | 65 | 75 |
| F88 | 33 | 44 | 46 | 68 | 75 | 80 |

ments an increase in core radius and aggregation number is expected. Assuming that the core consists essentially of liquid-like PPO (with some water; the solubility of water in PPO at room temperature is about 5%) the core radius can be used for an estimation of the aggregation numbers. The volume of a PO unit is about 95 Å$^3$; increasing this value to 100 Å$^3$ allows for the presence of 5% of water. The P85 micelle, at 40 °C, should then contain 115 monomers, if the core radius is 47.7 Å as in Table 3. Mortensen and Pedersen [42] suggested that the PO core is surrounded by a monolayer of densely packed EO-units. Reducing the core radius by 4 Å to allow for this reduces the aggregation number to 90. These values are not consistent with the measured aggregation number from TRFQ of only 60 (and that from SLS is even lower). The conclusion is then that the core cannot be composed of only PO-blocks.

Using the core radius from SANS (Table 3) and the aggregation number at the same temperature from fluorescence quenching, Fig. 11, the composition of the core can be estimated. We assume that the core volume comprises all PO-groups, i.e., 39 per unimer in the case of P85, and an unknown number, $x$, of EO-groups per unimer; we also assume that there is one water per EO group. Equating the core volume calculated from the core radius with the sum of the group volumes, $x$ can be determined from

$$4/3\pi R_c^3 = N_{agg}(39V_{PO} + x(V_{EO} + V_{aq})) . \quad (1)$$

Using $V_{PO} = 95.5$ Å$^3$, $V_{EO} = 72.5$ Å$^3$, and $V_{aq} = 30$ Å$^3$ we obtain $x = 34$, and the ratio $(EO/PO)_{core} = 0.87$. Assuming instead as much as two water molecules per EO in the core, the EO/PO ratio is reduced to 0.67. $R_c = 55$ Å and $N_{agg} = 95$ and 60 °C give for the ratio 0.90 with one, and 0.69 with two water molecules per EO.

These results are in agreement with the picture of the distribution of EO and PO segments from the calculations by Linse [25], reproduced in Fig. 7. Both the distributions are broad. The PO distribution starts at an almost constant level and decays in a broad slope with a half-value and inflexion point at about the same distance from the center as where the EO distribution has its peak. If, in the simple core-mantle model, the core radius is taken as the radius where the total segment density is half maximum

(about 12 layers in Fig. 7), then it is apparent that a considerable fraction of the EO segments would be included in the core as well. A rough estimate for the case modeled in Fig. 7 ($E_{99}P_{65}E_{99}$) at a polymer volume fraction of 5%, 15° above the CMT, shows that 62 PO and 53 EO segments from each monomer are found within the core, and in addition water (probably strongly overestimated [28]). The ratio $(EO/PO)_{core}$ is obtained as 0.85, in good agreement with the estimate for P85, assuming one water molecule per EO. The close agreement is of course fortuitous, but indicates nevertheless that the concept of a core containing considerable amounts of EO segments and water seems to be viable. Furthermore, with such a core the PO blocks can be accomodated in large micelles without being unduly constrained to stretched states.

Linse [25] also calculated the hydrodynamic radius from the segment distributions. In the case discussed the hydrodynamic radius was 20 layers, or a factor of 1.67 larger than the core radius as defined above. The ratios from the results collected in Tables 2 and 3 (using values for 50 °C for F87 and F88, since this is about 20 °C above the CMT) are 1.6, 1.7, and 2.2 for P85, F87, and F88, respectively. The segment distributions resulting from the model calculations may therefore give a good picture of the structure of the real micelles. Stretching the comparison even further, we may ask what segment density correspond to the hard-sphere interaction radius used in the interpretation of the SANS results. The SANS data correspond to a hard-sphere to core ratio of about 1.5. This ratio would locate the hard-sphere interaction radius at 18 layers in the model, where the segment volume fraction is about 0.1, with almost exclusively EO segments. Interpenetration of the two distributions to this depth would certainly result in a strong and steeply rising repulsion.

## Rod-like micelles

In the original P85 study [36], the DLS measurements were performed below the temperature at which a change to long micelles could be expected from the change in the rheological behavior. Later DLS measurements clearly demonstrated the formation of rods, and at very low concentrations the length of the cylinders has been determined from the rotational component in the relaxation spectrum [14, 16]. At higher temperatures ($T > 70$ °C for P85) in dilute solution (concentration less than about 1%) the micelles become elongated and the viscosity increases strongly up to the clouding temperature. This trend is also shown by the total intensity of scattered light. The aggregation number from the molecular weight obtained using total intensity light scattering as well as from fluorescence decay measurements also increases above about 70 °C, as discussed above in conjunction with Fig. 11. Viscoelastic measurements show the presence of a soft "gel" down to 1–2% at high temperatures, attributed to hindered rotation of overlapping rods. Estimates were made of the length of the rods (or extended ellipsoids) formed in this higher temperature range at very low concentrations using dynamic polarized light scattering and also depolarized light scattering [16].

Figure 12a shows a typical correlation function for a dilute solution of P85. The low amplitude fast peak (relaxation rate $\Gamma_f$) seen in the corresponding inverse Laplace transform (ILT) in Figure 12b is due to a mixture of the rotational diffusion and translational diffusion and appears as the second term on the right in the equation:

$$g^{(1)}(t) = S(q,t) = S_0(qL)e^{-q^2Dt} + S_1(qL)e^{-(q^2D+6\Theta)t} + \cdots, \quad (2)$$

where the $S_0$ term describes the translational diffusion, $t$ is the time, $q$ the scattering vector, $L$ the length of the rod,

**Fig. 12** Autocorrelation function of the polarized scattered light at 120° (a) and the corresponding relaxation time distribution obtained from inverse Laplace transformation (b) for a dilute solution (0.024 wt%) of P85 in water at 75 °C. The small fast peak is related to the rotational motion and the slow to the translational motion of the rod-like micelle. (Reproduced with permission from ref. [16]

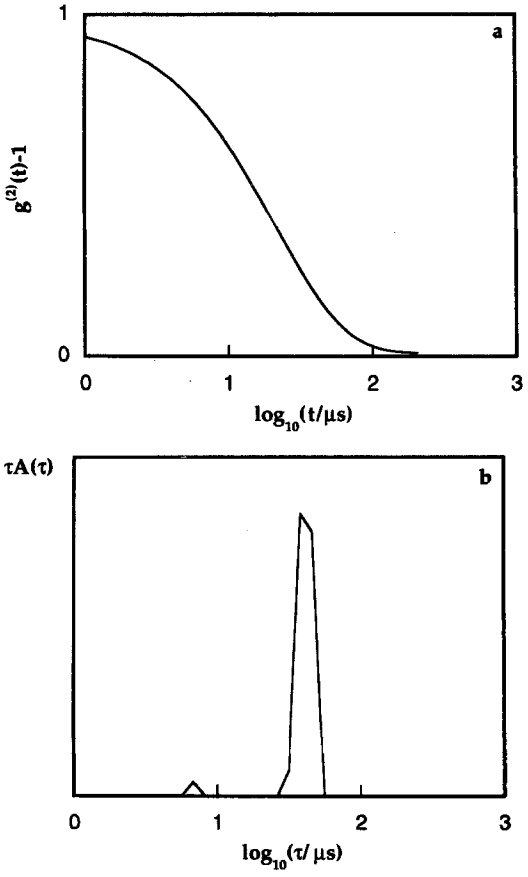

and $\Theta$ the rotational diffusion coefficient. Plots of the relaxation rate derived from the ILT result are shown for the two modes in Fig. 13. The linear plot is data for the slow translational mode while the curve describes the increasing amplitude of the higher terms in Eq. (3) which come into play as the scattering vector is increased.

Thus, from the value of $\Gamma_f = (q^2D + 6\Theta)$ at $q = 0$, one obtains the rotational diffusion coefficient $\Theta$. Use is then made of Broersma's equations for rigid rods [45] which give $L$ in terms of the rotational diffusion coefficient. We obtain the average value $L = 1020$ Å. Note that since the micellar diameter is 150 Å (using the radius of the spherical micelle at lower temperatures) $L/d \approx 7$.

From the translational diffusion coefficient one obtains $R_H = 247$ Å, a value which can be compared with model expressions. The experimental value lies between that for a rod (285 Å) and that for a prolate ellipsoid (213 Å).

From the length and diameter one can estimate, using standard expressions, a value for the radius of gyration of $R_g = 310$ Å. Thus, $\rho = (R_g/R_H) \approx 1.25$, which is intermediate between the theoretical values for a sphere (0.778) and a rod ($\rho > 2.0$), reflecting the fact that the micelle is short and bulky.

At around 70 °C the micellar solutions show significant depolarized intensity. This is due mainly to the non-spherical shape of micelle (i.e., to the form anisotropy) since the depolarized intensity is negligible at lower temperatures at which only spherical micelles are present.

Measurements of the polarized scattering as a function of temperature show that the rod-like micelles grow with increasing temperature. The length is about 1200 Å at 80 °C and 1700 Å at 85 °C ($L/d \approx 11.3$). Clouding occurs at about 87 °C in this low concentration range.

**Fig.13** The relaxation rates of the two modes shown in Fig. 12b plotted as a function of the square of the scattering vector, for 0.05 wt% P85 at 75 °C. The slow mode is proportional to $q^2$ and the slope gives the translational diffusion coefficient. The rotational diffusion coefficient is given by the value at $q = 0$ from the fast rate. (Reproduced with permission from ref. [16])

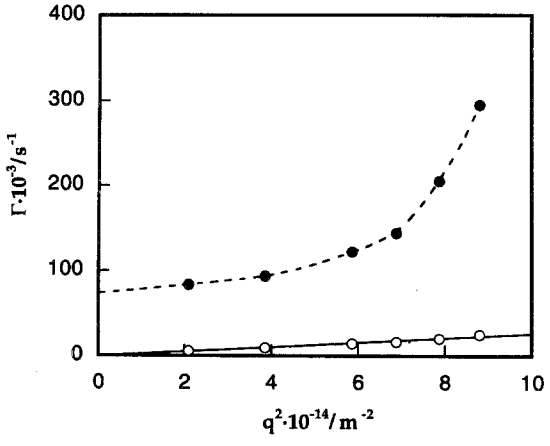


## Effect of salt and ionic surfactants

The effect of salt on the clouding behavior of Pluronic solutions is similar to that observed for nonionic surfactants of the $C_xE_y$-type, and for PEO itself in aqueous solution [46]. Qualitatively, a lowering of the cloudpoint is observed except for salts with large polarizable anions, like $SCN^-$, and $I^-$, where an initial increase is often noted. The effectiveness of various ions in lowering the cloud point follows the lyotropic series, and the effect is often discussed in terms of "salting in" and "salting out," of "structure-making" and "structure-breaking" additives. The former concept is entirely descriptive, and adds nothing to the understanding of the phenomenon, whereas the latter is false, since closely similar effects are also obtained in polar solvents like formamide, with an entirely different structure. This was pointed out by Karlström et al. [18, 47] in a recent discussion of the salt effects, based on the model of the EO-chain as having two classes of conformers with different polarity, and different interaction energies with a polar solvent. A simple but effective approach was used to qualitatively predict the effects of additives: those that increase the polarity difference between the solvent and the polymer will favor phase separation and decrease the cloud temperature. Salts like NaCl and KF are depleted in the immediate vicinity of the polymer coil with its low polarizability, and increase the polarity of water (and a solvent like formamide). Phase separation is facilitated and the cloud point depressed. In salts like NaI, on the other hand, the large, polarizable anion seems to partition slightly in favor of the polymer, increasing its polarity and thereby reducing the polarity difference. The polymer becomes more compatible with the solvent, and the cloud point is increased.

An anionic surfactant like SDS has an even stronger tendency to adsorb onto the polymer chain, either as monomers, or more often, as small micelle-like clusters. Two effects result: On the one hand, charges are introduced on the chain and give rise to long-range electrostatic repulsion, which keeps the polymer coils expanded and away from each other, thus increasing the cloudpoint. On the other hand, the surfactant molecules or micelles may bind to more than one polymer coil, thus introducing an effective bridging between the polymers. The electrostatic effect dominates at low salt concentrations. Addition of salt screens this interaction, and results in an attractive interaction between the polymer and the surfactant. At low surfactant concentrations small amounts of added salt

gives a dramatic, synergistic lowering of the cloud point [48]. At higher surfactant concentrations the repulsive interactions between micelles become important, which again results in an increase of the clouding temperature.

The effects of salts on the clouding behavior of various Pluronic copolymers are well explained in this way [47]. Salts such as KF lower the cloud point strongly [9]. It is also observed that some of the rheological transition temperatures are lowered to the same extent, e.g., the transition to a "gel" of long micelles below the cloudpoint, discussed above in conjunction with Fig. 1. Furthermore, for both P85 and L64 the intrinsic viscosity was found to follow the same universal curve when plotted vs $T-T_c$, at different concentrations of KCl and KF [9]. The rheological properties are related to the size, shape, and interactions of the micelles in the solution. Changes in these parameters, as well as in the cloudpoints, should be largely determined by changes in the effective interactions of the exposed EO-blocks of the copolymer micelles. Whether addition of salt causes the whole phase diagram to be displaced along the temperature scale remains to be seen.

The onset of micelle formation is also lowered by salt addition, but is much less affected than the cloud point [49]. Micelle formation depends mainly on the hydrophobicity of the PPO-blocks, which is already large without salts present and not so much affected by a further increase of the polarity difference between the polymer and the solvent; a comparatively small effect in this case is thus understandable.

The influence of SDS on micelle formation for two Pluronics, F68 and L64, has been investigated [40]. F68 is a very hydrophilic material, which does not form micelles on its own at 40 °C, whereas L64 forms micelles at this temperature but not at 20 °C. It was observed – from fluorescence quenching experiments – that addition of very low concentrations of SDS induces micelle formation at both temperatures. Small micelles comprising 4–5 copolymer molecules and about 20 SDS molecules seem to form first, with free copolymers present simultaneously. With the addition of more surfactant, more copolymer becomes solubilized in the small micelles – at 1% F68 and 3.5 mM SDS all the copolymer is present in micelles. On further addition of SDS the micelles grow with respect to SDS, but with fewer copolymers per micelle, and approach the size and properties of free SDS micelles at high surfactant concentration.

For L64 at 40 °C the fluorescence method indicates the presence of large micelles, comprising about 70 monomers, deduced after correction for free polymers as mentioned above. Addition of SDS reduces the size of the micelles until, after addition of about 0.3% w/w SDS (10 mM) to 1% L64 (3.4 mM), the micelles are similar to those obtained on addition of SDS to unmicellized L64 at 20 °C. With further addition the micelles grow as SDS forms micelles with solubilized copolymer at both temperatures.

The strong effect of SDS on the micellization of the Pluronics is also apparent from measurements of $^{13}C$ NMR chemical shifts of the methyl carbons of the PO blocks [40] (see Fig. 14). At 40 °C there is a down-field shift of 0.88 ppm due to micellization: this is the difference between the chemical shifts for the methyl carbons of the PPO blocks in unmicellized F68 and in micellized L64. Neat PPO shows a shift similar to that for F68 in water. Addition of as little as 0.2% of SDS to 1% of F68 gives a downfield shift of about 0.4 ppm; this shift is only slightly changed on further addition of SDS, and is the same as that noted for 1% L64 with more than 1% of SDS. Addition of low concentrations of SDS to micellar L64 rapidly reduces the initial downfield shift of 0.88 ppm to this level. Since the $^{13}C$ shifts are believed to be mainly due to the conformational state of the C–C bond, the interpretation offered is that the variation of the shifts indicates changes in packing and extension of the PO-blocks, which affects their conformations. The large down-field shift in L64 on micellization is taken as an indication that the PO-blocks in these large micelles are much more extended than in the neat copolymer, and partly relaxes when the smaller mixed micelles are formed [40].

It is obvious from these results that the ionic surfactant interacts strongly with the non-polar PO-blocks of the copolymers, and enhances the attraction between them. Simultaneously, charges are introduced on the resulting

**Fig. 14** $^{13}C$ NMR chemical shifts for the methyl carbons in the PO blocks of L64 and F68 in 1 wt% aqueous solutions at 40 °C, as a function of added concentration of SDS. The shifts are given in ppm relative to the shift for 1 wt% F68 without SDS. F68 is then in monomeric form. The shift for neat PPO, indicated by the arrow, is close to that value, whereas micellized L64 is shifted downfield by 0.88 ppm. (Replotted with permission from data in ref. [40]. Copyright [1991] American Chemical Society)

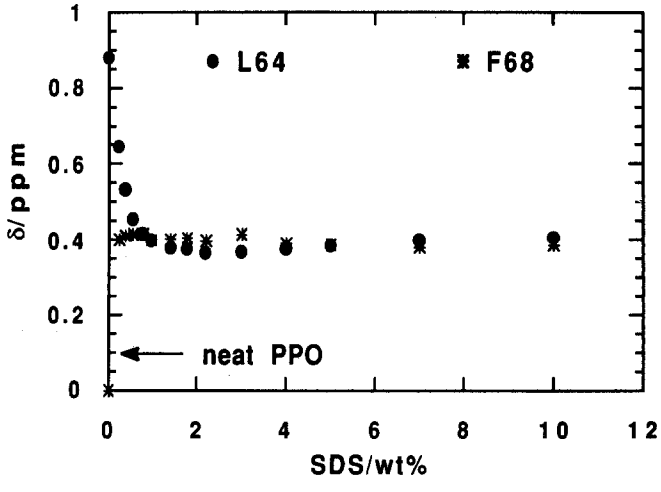

mixed micelles, which favors the formation of relatively small curved aggregates.

## Conclusion

A detailed knowledge of the phase behavior and aggregation properties of block copolymers of the EO-PO-EO type in aqueous environments is emerging from experimental and theoretical efforts. With the great variability of composition of these useful copolymers there are still many interesting and important systems to be explored. More phase diagrams with higher precision are required, and the high temperature and water poor regions remain to be explored. A SANS and light scattering study of P85 melts and concentrated solutions $p$ at high temperature has been initiated (50). There is also a need for a more detailed picture of the micelles, e.g., the PO-EO distribution throughout the core and mantle, and how it changes with temperature. Such information would at least in principle be possible to obtain from SANS measurements on selectively deuterated compounds.

## References

1. Lindman B, Thalberg K (1993) in: Goddard ED, Ananthapadmanabhan KP (eds) Interactions of Surfactants with Polymers and Proteins; eds. CRC Press, Boca Raton, 1993; Chapter 5
2. Piculell L, Lindman B (1992) Adv Colloid Interface Sci 41:149
3. Tuzar Z, Kratochvil P (1976) Adv Colloid Interface Sci 6:201
4. Hurter PN, Scheutjens JMHM, Hatton TA (1993) Macromolecules 26:5030 and 5592
5. Glatter O, Scherf G, Schillén K, Brown W (1994) Macromolecules 27:6046
6. Hvidt S, Jørgensen EB, Brown W, Schillén K, J Phys Chem (in press)
7. Mortensen K (1992) Europhysics Lett 19:599
8. Tiddy G, private communication
9. Bahadur P, Pandya K, Almgren M, Li P, Stilbs P (1993) Colloid Polymer Sci 271:657
10. Lindblad C, Schillén K, Almgren M (to be published)
11. Glatter O (1993) J Physique (France) IV, 3, C1–27
12. Tanford C (1980) "The Hydrophobic Effect", J Wiley, New York
13. Brown W, Schillén K, Hvidt S (1992) J Phys Chem 96:6038
14. Mortensen K, Brown W (1993) Macromolecules, 26:4128
15. Almgren M, Bahadur P, Jansson M, Li P, Brown W, Bahadur A (1992) J Colloid Interface Sci, 151:157
16. Schillén K, Brown W, Johnsen RM (1994) Macromolecules, 27:4825
17. Mortensen K, Schwar D, Jansen S (1993) Phys Rev Lett 71:1728
18. Kjellander R, Florin E (1981) J Chem Soc Faraday Trans I, 77:2053
19. Karlström G, Carlsson A, Lindman B (1990), J Phys Chem 94:5005
20. Saeki S, Kuwahara N, Nakat M, Kaneko M (1976) Polymer 17:685
21. Karlström G (1985) J Chem Phys, 89:4962
22. Andersson M, Karlström G (1985) J Chem Phys 89:4957
23. Björling M, Karlström G, Linse P (1991) J Phys Chem, 95:6706
24. Malmsten M, Linse P, Zhang K-W (1993) Macromolecules, 26:2905
25. Linse P (1993) Macromolecules, 26:4437
26. Linse P, Björling M (1991) Macromolecules, 24:6700
27. Scheutjens JMHM, Fleer GJ (1979) J Phys Chem 83:1619; Ibid (1980) 84:178
28. Linse P, Malmsten M (1992) Macromolecules 25:5434
29. Linse P (1993) J Phys Chem 97:13869
30. Tiberg F, Malmsten M, Linse P, Lindman B (1991) Langmuir 7:2732
31. Linse P (1994) Macromolecules 27:2685
32. Linse P (1994) Macromolecules, 27:6404
33. Turro NJ, Kuo PL (1986) Langmuir 2:438
34. Almgren M, Alsins J, Bahadur P (1991) Langmuir 7:446
35. Zhou Z, Chu B, (1987–88) Macromolecules 20:3089; Ibid 21:2548
36. Brown W, Schillén K, Almgren M, Hvidt S, Bahadur P (1991) J Phys Chem 95:1850
37. Stilbs P (1986) Progr in NMR Spectroscopy 19:1–45
38. Zhou Z, Chu B (1988) J Colloid Interface Sci 126:171
39. Warr GG, Grieser F, Healy TW (1983) J Phys Chem 87:1220
40. Almgren M, van Stam J, Lindblad C, Li P, Stilbs P, Bahadur P (1991) J Phys Chem 95:5677
41. Mortensen K, Brown W, Nordén B (1992) Phys Rev Lett 68:2340
42. Mortensen K, Pedersen JS (1993) Macromolecules, 26:805
43. Pusey PN, van Megen W (1986) Nature 320:340
44. Hoover WG, Ree FH (1968) J Chem Phys 49:3609
45. Broersma S (1960) J Chem Phys 32:1626 and 1632; Ibid (1981) 74:6989
46. Florin E, Kjellander R, Eriksson JC (1984) J Chem Soc Faraday Trans I 80:2889
47. Samieh AA, Karlström G, Lindman B (1991) Langmuir 7:1067
48. Carlsson A, Karlström G, Lindman B (1986) Langmuir 2:536
49. Bahadur P, Li P, Almgren M, Brown W (1992) Langmuir 8:1903
50. Mortensen K, Brown W, Macromolecules (in press).